

# Energy Transfer by Way of an Exciplex Intermediate in Flexible Boron Dipyrromethene-Based Allosteric Architectures

Soumyaditya Mula,<sup>†</sup> Kristopher Elliott,<sup>‡</sup> Anthony Harriman,<sup>\*,‡</sup> and Raymond Ziessel<sup>\*,†</sup>

Laboratoire de Chimie Organique et Spectroscopies Avancées (LCOSA), Ecole Européenne de Chimie, Polymères et Matériaux, Université de Strasbourg, 25 rue Becquerel, 67087 Strasbourg Cedex 02, France, and Molecular Photonics Laboratory, School of Chemistry, Bedson Building, Newcastle University, Newcastle upon Tyne NE1 7RU, United Kingdom

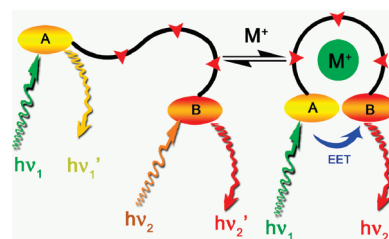
Received: July 16, 2010; Revised Manuscript Received: August 30, 2010

We have designed and synthesized a series of modular, dual-color dyes comprising a conventional boron dipyrromethene (Bodipy) dye, as a yellow emitter, and a Bodipy dye possessing extended conjugation that functions as a red emitter. A flexible tether of variable length, built from ethylene glycol residues, connects the terminal dyes. A critical design element of this type of dyad relates to a secondary amine linkage interposed between the conventional Bodipy and the tether. Cyclic voltammetry shows both Bodipy dyes to be electroactive and indicates that the secondary amine is quite easily oxidized. The ensuing fluorescence quenching is best explained in terms of the rapid formation of an intermediate charge-transfer state. In fact, exciplex-type emission is observed in weakly polar solvents and over a critical temperature range. In the dual-color dyes, direct excitation of the yellow emitter results in the appearance of red fluorescence, indicating that the exciplex is likely involved in the energy-transfer event, and provides for a virtual Stokes shift of 5000  $\text{cm}^{-1}$ . Replacing the red emitter with a higher energy absorber (namely, pyrene) facilitates the collection of near-UV light and extends the virtual Stokes shift to 8000  $\text{cm}^{-1}$ . Modulation of the efficacy of intramolecular energy transfer is achieved by preorganization of the connector in the presence of certain cations. This latter behavior, which is fully reversible, corresponds to an artificial allosteric effect.

## Introduction

The successful realization of artificial photosynthesis,<sup>1</sup> whereby sunlight is converted to chemical potential in abiotic but bioinspired molecular arrays, requires the close cooperation between two separate photosystems.<sup>2</sup> The first such system must collect photons across a broad spectral range before directing the harvested electronic energy to a remote site. The second photosystem drives successive electron-transfer reactions aimed at fuel production.<sup>3</sup> Although in principle it should be possible to design integrated chemical networks based on a single photosystem, it seems most unlikely that any single chromophore will possess the optimal features for both photon collection and electron transfer.<sup>4</sup> As such, we have focused attention on the light-harvesting apparatus<sup>5</sup> and designed several rigid arrays capable of absorbing light over most of the visible range.<sup>6</sup> These systems display highly efficient energy transfer among disparate chromophores until concentrating the excitation energy at a terminal acceptor. Various transfer mechanisms coexist but can be resolved by way of ultrafast fluorescence spectroscopy. At a purely fundamental level, some of these systems can be used to test the validity of Förster's theory of electronic energy transfer at short separation distances<sup>7</sup> and to better define the resistance of molecular-scale wires for conducting electronic charge.<sup>6a</sup> It is notable that minor alteration of the conformation or composition of the system can cause an important perturbation of the energy-transfer rates.<sup>8</sup>

## CHART 1: Simple Illustration of an Artificial Allosteric Effect As Applied to Intramolecular EET in a Two-Color Dye Caused by Introduction of a Cation ( $M^+$ ) Able To Bind to the Connecting Tether



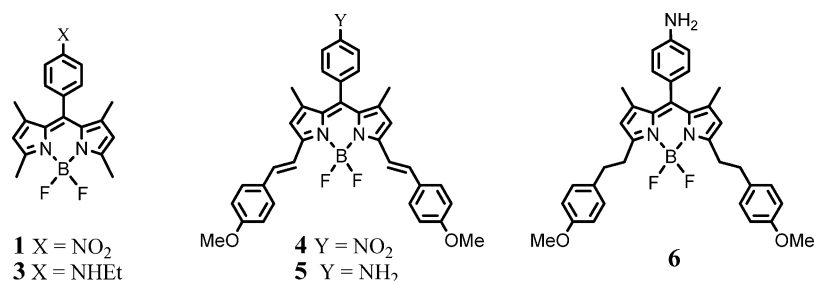
A particular problem associated with this rational approach to the construction of abiotic photon collectors relates to the protracted synthesis needed to bring about an energy-transfer cascade.<sup>6</sup> While interesting from an elementary viewpoint, such an elaborate synthesis presents difficulties for scaleup and/or repair of damaged modules. Replacing the rigid connectors with flexible analogues might simplify the preparative aspects but tends to curtail through-bond electron exchange.<sup>9</sup> This means that energy transfer must occur via the Förster dipole–dipole mechanism,<sup>10</sup> for which the choice of chromophore is more restricted. A potential way around this specific problem might be to impose some kind of allosteric effect<sup>11</sup> on the connecting chain, as illustrated in Chart 1. Allosterism, either positive or negative, is ubiquitous in nature, where biological events must be regulated toward chemical or physical stress from the outside world.<sup>12</sup> The simple concept introduced here is to link two dyes, each based on difluoroboradiaza-*s*-indacenes, commonly termed Bodipy, having different colors and being linked by a polyeth-

\* To whom correspondence should be addressed. E-mail: anthony.harriman@ncl.ac.uk (A.H.); ziessel@unistra.fr (R.Z.).

<sup>†</sup> Université de Strasbourg.

<sup>‡</sup> Newcastle University.

## CHART 2: Reference Compounds Used To Aid Understanding of the Redox and Optical Properties



ylene glycol chain. Electronic energy transfer (EET) between the terminals should be promoted by folding the chain into a closed conformation.

In seeking to involve the connecting chain in the transfer process, something other than a cation-induced folding process might be necessary. Now, earlier work<sup>13</sup> has shown that a fluorescent charge-transfer state could be formed from a Bodipy dye equipped with a weak redox-active unit at the meso position. The latter site is crucial because of the need to hold the reactants in an orthogonal geometry.<sup>14</sup> We now consider the possibility to use such an intermediate as a relay for intramolecular energy transfer. Since it is well-known<sup>15</sup> that an amine will form a fluorescent exciplex with many different types of aryl polycycles, a logical starting point would seem to hinge on the design of a molecular architecture comprising two disparate Bodipy dyes, an allosteric chain and a meso-linked arylamine. To properly test the idea, chains of differing length are required. We now expand on this generic idea and describe intramolecular energy transfer taking place in molecular systems subjected to exciplex formation.<sup>16</sup> There are few, if any, reported cases where an exciplex is directly involved in energy transfer.<sup>17</sup>

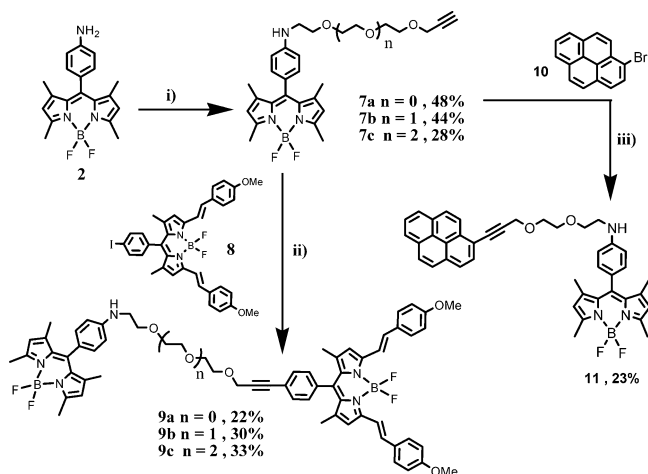
## Results and Discussion

The routine synthesis and characterization of the reference compounds sketched in Chart 2 are described in the Supporting Information.

The synthesis of the target compounds involves alkylation of the amino group of 4,4-difluoro-1,3,5,7-tetramethyl-8-anilino-4-bora-3a,4a-diaza-*s*-indacene (**2**) with a polyethylene glycol-based reagent bearing two disparate functionalities: The tosylate derivative is known to facilitate nucleophilic substitution, whereas the propargylic function provides the reactive site needed for cross-linking to aryl-based residues via a palladium-promoted reaction. A biphasic reaction in water using NaHCO<sub>3</sub> as the base, 1,2-dichloroethane as the nonmiscible solvent, and dodecyl sulfate as the phase transfer agent was found to provide the best conditions (Scheme 1). Though the yield was modest, the reaction furnished the mono-*N*-substituted products **7a–7c**, but with a linker suitable for subsequent substitution chemistry.

To obtain the target compounds and to explore the synthetic versatility of compounds **7a–7c**, the isolated derivatives were subjected to cross-coupling with 4,4-difluoro-3,7-bis(*p*-methoxystyryl)-1,7-dimethyl-8-(*p*-iodophenyl)-4-bora-3a,4a-diaza-*s*-indacene (**8**). Specifically, Sonogashira coupling reactions promoted by palladium(0) were employed to furnish **9a–c** in satisfactory yield (Scheme 1). Finally, dye **7a** was treated with 1-bromopyrene (**10**) to obtain the flexibly linked pyrene derivative **11**.

**Electrochemistry.** Selected electrochemical properties measured for **3**, **7a**, **8**, and **9a** are gathered in Table 1. For each compound, one reversible cathodic wave was observed in the cyclic voltammograms and assigned to the one-electron reduc-

SCHEME 1<sup>a</sup>

<sup>a</sup> Reagents and conditions: (i) aqueous NaHCO<sub>3</sub>, dodecyl sulfate, corresponding tosylate, C<sub>2</sub>H<sub>4</sub>Cl<sub>2</sub>, 80 °C, 24 h; (ii) [Pd(PPh<sub>3</sub>)<sub>4</sub>] (6 mol %), benzene, Et<sub>3</sub>N, 50 °C; (iii) [Pd(PPh<sub>3</sub>)<sub>4</sub>] (6 mol %), benzene, (iPr)<sub>2</sub>NH, 70 °C.

TABLE 1: Electrochemical Properties of Selected Dyes<sup>a</sup>

compd	$E_{\text{ox}}^{\circ}/V$ ( $\Delta E/\text{mV}$ )	$E_{\text{red}}^{\circ}/V$ ( $\Delta E/\text{mV}$ )
<b>3</b>	+1.04 (irrev); +1.21 (90)	−1.30 (70)
<b>7a</b>	+0.98 (irrev); +1.12 (90)	−1.27 (70)
<b>8</b>	+0.74 (60); +1.08 (70); +1.58 (irrev)	−0.97 (60); −1.90 (irrev)
<b>9a</b>	+0.72 (60); +0.98 (irrev); +1.11 (irrev); +1.22 (irrev); +1.57 (irrev)	−1.01 (70); −1.29 (74); −1.88 (irrev)

<sup>a</sup> Potential determined by cyclic voltammetry in deoxygenated CH<sub>2</sub>Cl<sub>2</sub> solutions, containing 0.1 M TBAPF<sub>6</sub>, at a solute concentration of (1–5) × 10<sup>−3</sup> M, at 20 °C. Potentials were standardized with ferrocene (Fc) as the internal reference and converted to SCE assuming that  $E_{1/2}(\text{Fc}/\text{Fc}^+) = 0.38$  V ( $\Delta E_p = 70$  mV) SCE. The error in half-wave potentials is ±10 mV. When the redox potential is irreversible, the peak potential ( $E_{\text{ap/cp}}$ ) is quoted. All waves are mono-electronic unless otherwise specified.

tion of the Bodipy unit;<sup>18</sup> the derived reduction potentials ( $E_{\text{red}}^{\circ}$ ) and separations between forward and reverse peaks ( $\Delta E$ ) are provided in Table 1. In the case of **8**, which bears two styryl arms, reduction is easier by ca. 300 mV compared to that of both **3** and **7a**, while there is a second reductive step that corresponds to formation of the  $\pi$ -dianion. In the anodic portion of the cyclic voltammograms, an irreversible peak is observed together with a reversible wave that could be assigned to one-electron oxidation of the Bodipy unit;<sup>18</sup> the respective oxidation potentials ( $E_{\text{ox}}^{\circ}$ ) and peak separations are also given in Table 1. The additional irreversible peak observed for **3** and **7a** is due to the one-electron oxidation of the secondary amine center; it is recognized that such processes are often irreversible.<sup>19</sup> As might be expected, the anodic portion of the cyclic voltammo-

**TABLE 2: Photophysical Properties of Selected Amino-Bodipy Dyes Recorded in Diethyl Ether at Room Temperature**

compd	$\lambda_{\text{abs}}/\text{nm}$	$\epsilon_{\text{max}}/\text{M}^{-1} \text{cm}^{-1}$	$\lambda_{\text{flu}}/\text{nm}$	$\Phi_{\text{F}}$	$\tau_{\text{S1}}/\text{ns}$	$\tau_{\text{S2}}/\text{ns}$
<b>2</b> <sup>a</sup>	500	80000	510	0.38	3.1	
<b>3</b>	500	86000	513	0.017	0.16	2.3
<b>5</b>	641	102000	656	0.32	5.8	
<b>6</b>	504	99000	514	0.38	3.0	
<b>7a</b>	500	103000	515	0.027	0.24	1.9
<b>7b</b>	500	98000	515	0.053	0.48	1.7
<b>7c</b>	500	74000	514	0.060	0.51	1.5

<sup>a</sup> All values for **2** were determined in anhydrous  $\text{CH}_2\text{Cl}_2$ .

gram recorded for **8** is more crowded than for the other compounds. On the basis of the electrochemical properties recorded for similar analogues of the distyryl dye, the first oxidation step is assigned to removal of one electron from the Bodipy unit. Two additional waves observed at higher potential are now assigned to oxidation of the styryl residue and to removal of a second electron from the Bodipy nucleus, respectively.

Interestingly, each of the anodic and cathodic waves observed for the precursors **7a** and **8** were present in the assembled dye **9a**. In particular, the two reversible, cathodic waves separated by 280 mV could be assigned to successive reduction of the two Bodipy-based terminals. These units are too remote to interact in an electronic sense or to offer electrostatic perturbations. The anodic portion of the voltammogram recorded for **9a** is crowded with waves, but the first two processes could be assigned to oxidation of the modified Bodipy nucleus and of the amine center, respectively. Similar cyclic voltammograms were recorded for the yellow dyes **7b** and **7c** and for the dual dyes **9b** and **9c**. These data are in keeping with a molecular dyad in which the two partners remain in electronic isolation.

**Photophysics of the Amino-Bodipy Dyes.** The primary amino derivatives **2** and **5** display absorption spectra typical of Bodipy units with the relevant degree of  $\pi$ -conjugation,<sup>20</sup> possessing intense absorption maxima ( $\lambda_{\text{max}}$ ) at 500 and 641 nm, respectively (Table 2). The molar absorption coefficients ( $\epsilon_{\text{max}}$ ) measured at the peak maxima are in line with values recorded for related compounds.<sup>20</sup> Both dyes fluoresce in solution, exhibiting clear emission maxima ( $\lambda_{\text{flu}}$ ) at 510 and 656 nm, respectively, with reasonably high quantum yields ( $\Phi_{\text{F}}$ ) measured at room temperature (Table 2). Fluorescence decay profiles remain monoexponential for both compounds and can be analyzed to obtain the corresponding emission lifetimes ( $\tau_{\text{S}}$ ), which are collected in Table 2. There is no indication for light-induced electron transfer in any solvent and no evidence for the involvement of charge-transfer states. Alkylation of the amino function, forming **3** (bearing an ethyl group) or **7a–c** (functionalized with polyethylene glycol residues of varying length) results in a pronounced decrease of  $\Phi_{\text{F}}$  in diethyl ether ( $\text{Et}_2\text{O}$ ) at room temperature (Table 2). Individual  $\Phi_{\text{F}}$  values show a modest sensitivity toward the length of the tether in  $\text{Et}_2\text{O}$  and increase slightly for longer chain lengths. In each case, the corrected excitation spectrum remains in good agreement with the absorption spectrum, the latter being little affected by alkylation. The reduced  $\Phi_{\text{F}}$  values are not a consequence of poor solubility or aggregation but are a genuine reflection of the system. Furthermore, the emission spectra recorded in  $\text{Et}_2\text{O}$  show the presence of an additional fluorescence profile centered at long wavelength that appears as a broad and featureless band (Figure 1). The emission spectral profile is independent of the sample concentration. Throughout this set of compounds, fluorescence decay profiles could not be analyzed satisfactorily in terms of single-exponential fits but followed dual-exponential

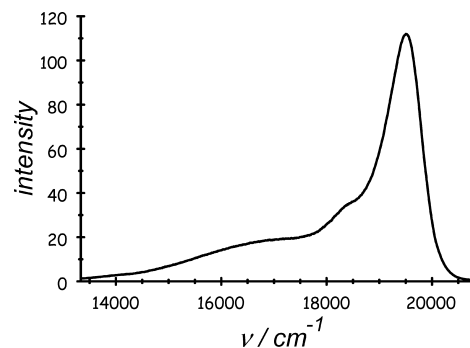


**Figure 1.** Fluorescence spectrum recorded for **7a** in diethyl ether at room temperature.

kinetics. The derived lifetimes,  $\tau_{\text{S1}}$  and  $\tau_{\text{S2}}$ , are collected in Table 2. To explore this behavior, detailed studies were undertaken with **7a** in a range of solvents.

The effect of the solvent polarity, as expressed in terms of the Pekar factor ( $f$ ), on the photophysical properties of **7a** are illustrated by the data compiled in Table 3. In cyclohexane, Bodipy-like emission is observed,  $\Phi_{\text{F}}$  remains similar to that observed for **2**, and decay curves are monoexponential at all monitoring wavelengths. A slight increase in  $f$ , however, leads to a decrease in  $\Phi_{\text{F}}$  and also in  $\tau_{\text{S}}$  and in the appearance of a structureless fluorescence band seen at long wavelength. This general behavior continues as  $f$  increases, and it is notable that, whereas  $\lambda_{\text{flu}}$  remains quite insensitive to changes in the nature of the solvent, the emission maximum for the longer wavelength band moves toward lower energy with increasing  $f$ . Both lifetimes decrease as  $f$  increases, although to differing degrees. A further feature of increasing  $f$  is that the featureless emission band becomes increasingly difficult to resolve from the baseline without using curve-fitting routines. This latter fluorescence band has the appearance expected for an emissive exciplex.<sup>21</sup> Monitoring at long wavelength leads to the conclusion that the exciplex decays via monoexponential kinetics with a lifetime closely comparable to  $\tau_{\text{S2}}$ . Critical examination of the emission from the Bodipy-like band around 515 nm indicates that this species decays via dual-exponential kinetics corresponding to  $\tau_{\text{S1}}$  and  $\tau_{\text{S2}}$  in all solvents except cyclohexane. Fitting the exciplex emission profile to a Gaussian band shape allows estimation of its quantum yield ( $\Phi_{\text{ex}}$ ) and the peak position ( $\nu_{\text{ex}}$ ), as can be seen from Table 3. There is a linear correlation between  $\nu_{\text{ex}}$  and  $f$ , as is often observed for emissive exciplexes,<sup>22</sup> with the notable exception of dioxane (Figure 2). Compounds **3**, **7b**, and **7c** show behavior remarkably similar to that summarized for **7a**.

Finally, temperature-dependence studies made in butyronitrile ( $\text{BuCN}$ ) show complex behavior. As mentioned above, fluorescence from the exciplex is difficult to resolve from the baseline at ambient temperature but becomes more pronounced on cooling (Figure 3). In fact, the exciplex emits strongly only

**TABLE 3: Effect of the Solvent Polarity on the Photophysical Properties of 7a Recorded at Room Temperature**

solvent	$f$	$\Phi_F^a$	$\tau_{S1}/ps$	$\Phi_{ex}$	$\tau_{S2}/ns$	$\nu_{ex}/cm^{-1}$
CHX <sup>b</sup>	0	0.46	4200			
dioxane	0.022	0.019	165	0.0070	1.34	16845
Bu <sub>2</sub> O <sup>c</sup>	0.097	0.115	1050	0.0090	2.05	17975
CHCl <sub>3</sub>	0.148	0.080	700	0.0080	1.80	17285
Et <sub>2</sub> O	0.163	0.027	240	0.0065	1.75	17125
EtOAc <sup>d</sup>	0.200	0.006	85	0.0041	1.70	16065
MTHF <sup>e</sup>	0.203	0.005	52	0.0029	1.54	15850
THF <sup>f</sup>	0.209	0.005	43	0.0025	1.35	15690
CH <sub>2</sub> Cl <sub>2</sub>	0.215	0.008	70	0.0020	1.20	15820
CH <sub>2</sub> ClCH <sub>2</sub> Cl	0.221	0.003	50	0.0016	0.96	15850
BuCN	0.281	0.002	41	0.0009	0.65	14550
CH <sub>3</sub> CN	0.305	0.002	37	0.0005	0.48	13800

<sup>a</sup> Refers to fluorescence from the S<sub>1</sub> state of the Bodipy unit. <sup>b</sup> Cyclohexane. <sup>c</sup> Dibutyl ether. <sup>d</sup> Ethyl acetate. <sup>e</sup> Methyltetrahydrofuran. <sup>f</sup> Tetrahydrofuran.

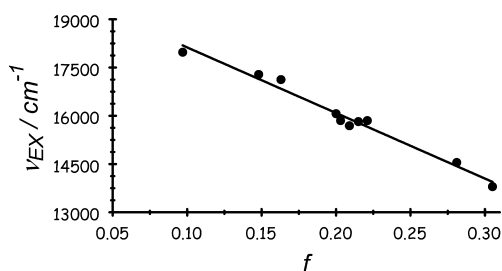


**Figure 2.** Effect of the solvent polarity on the maximum of the exciplex-like emission band. Note that the point for dioxane has been omitted.

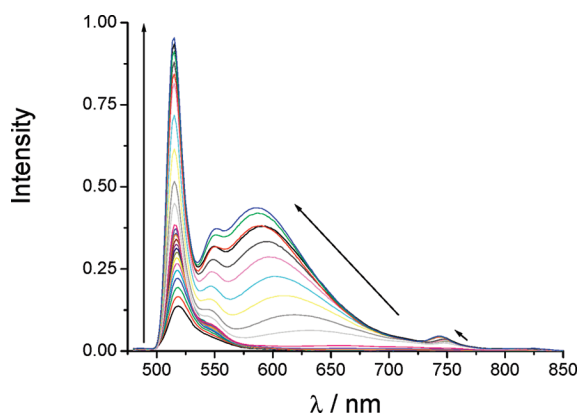


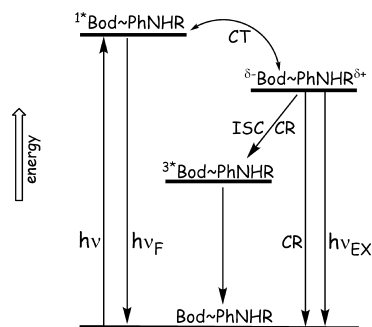
**Figure 3.** Effect of lowering the temperature on the emission spectrum recorded for 7a in butyronitrile. The arrow indicates the spectral shifts as the temperature decreases from 295 to 77 K.

as the temperature approaches the freezing point of the solvent, and over the same temperature range,  $\nu_{ex}$  moves sharply toward higher energy. This situation is consistent with freezing of the solvent, causing a significant decrease in the magnitude of  $f$ ,<sup>23</sup> specifically because the dielectric constant changes precipitously as the density of the solvent increases.<sup>24</sup> Surprisingly, exciplex emission is observed for 7a in a frozen glass at 77 K. Under identical conditions, Bodipy-like fluorescence increases in intensity without undergoing a substantial change in  $\lambda_{flu}$ . The absorption spectrum shows only a slight (i.e., 3 nm) blue shift and band narrowing over the same temperature range. At 77 K,  $\Phi_{ex}$  reaches a maximum value of 0.19 while  $\Phi_F$  increases to only 0.03; the low  $\Phi_F$  indicates that charge transfer still occurs in the glassy matrix at 77 K. Similar behavior is observed for 3, 7b, and 7c under comparable conditions, and exciplex fluorescence is found in BuCN near and below the freezing point.

The emission lifetimes were recorded for 7b under identical conditions. Starting first with  $\tau_{S2}$ , this being the fluorescence lifetime of the exciplex, we find that this parameter decreases slightly with decreasing temperature due to the accompanying increase in  $f$ . This effect is kept small, however, because of the offsetting inhibition of thermal repopulation of the Bodipy S<sub>1</sub> state. As the temperature approaches 165 K, which corresponds to the freezing point of BuCN, there is a sharp increase in  $\tau_{ex}$  that continues until vitrification of the solvent. At 77 K,  $\tau_{ex}$  reaches a maximum value of 34 ns. Over the same temperature range,  $\tau_{S1}$ , which can be taken to represent the lifetime of the Bodipy S<sub>1</sub> state, decreases from 41 ps at room temperature to 34 ps at 170 K and then begins to increase in line with the changes in  $f$ . At 77 K,  $\tau_{S1}$  attains a value of 250 ps. Monitoring at 515 nm, where the exciplex does not emit, shows that the fractional contribution made by the longer lived component becomes progressively less significant as the temperature falls. Such behavior is to be expected if the S<sub>1</sub> state and the exciplex are in thermal equilibrium.<sup>25</sup> Because of the temperature-induced changes in  $f$ , it is not possible to comment on whether charge transfer is thermally activated.

On the above basis, we assign the short-lived emission to the S<sub>1</sub> state localized on the Bodipy fluorophore while the longer-lived species is attributed to an exciplex intermediate. The latter is weakly emissive, except in low-polarity solvents or in a frozen glass. At room temperature in CH<sub>2</sub>Cl<sub>2</sub> electrochemical data can be used to conclude that intramolecular electron transfer to the first excited singlet state of the Bodipy unit is highly unlikely in 2 and 5. Alkylation lowers the oxidation potential of the amine and thereby brings the energy of the exciplex closer to that of the excited state, especially for 7a–c. The length of the tether is not expected to affect the energy of the exciplex, although there are small perturbations of the peak potential for the anodic wave (Table 1) among these derivatives.

We can rationalize the photophysical properties in terms of Scheme 2, where the exciplex plays a key role. Thus, excitation of the Bodipy chromophore in 3 or 7a–c in a weakly polar solvent results in fast charge transfer from the lone pair on the amino group to the excited state. The resultant exciplex is relatively long lived and able to repopulate the S<sub>1</sub> state by way of setting up a thermal equilibrium. The rates of formation and decay of the exciplex in Et<sub>2</sub>O, and also in BuCN, show a moderate dependence on the length of the tether (Table 2). This latter effect is most likely associated with a conformational change that must accompany exciplex formation.<sup>16,26</sup> Indeed, it is known that the maximum stabilization of the exciplex will occur when the lone pair is aligned with the  $\pi$ -orbitals on the

**SCHEME 2: Proposed Pathways for Deactivation of the Bodipy Excited Singlet State Following Selective Excitation<sup>a</sup>**


<sup>a</sup> CT = charge transfer, CR = charge recombination, and ISC = intersystem crossing.

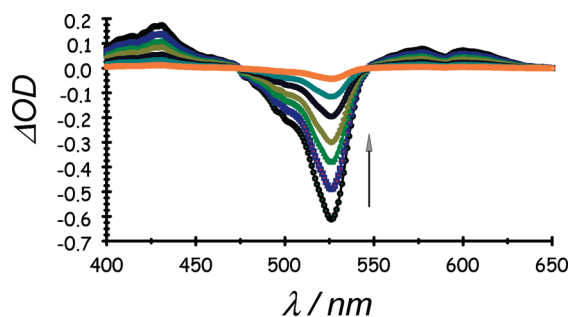


**Figure 4.** Triplet-triplet differential absorption spectra recorded after laser excitation ( $\lambda = 490$  nm; fwhm = 4 ns) of **7a** in deoxygenated butyronitrile at room temperature. Individual traces were recorded at different times after the excitation pulse.

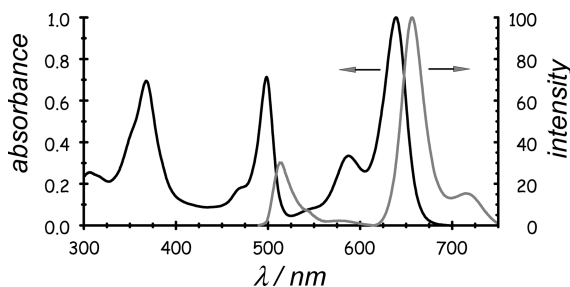


**Figure 5.** Absorption (black curve) and fluorescence (gray curve) recorded for **9a** in diethyl ether at room temperature. The excitation wavelength was 490 nm.

benzene ring,<sup>27</sup> and this requires that a subtle geometry change accompanies hybridization of the N atom.<sup>28</sup> Decay of the exciplex results in partial formation of the Bodipy-based triplet excited state, as detected by nanosecond laser flash photolysis in deoxygenated BuCN (Figure 4).

**Energy Transfer between the Terminals.** Having established the photophysics of the secondary amino derivatives of the yellow-emitting Bodipy unit, attention now turns to the possibility of engineering EET to the red-emitting Bodipy derivative. For the dual dyes **9a–c**, the absorption spectra appear as linear combinations of the absorption bands of the individual components while fluorescence can be detected from both terminals (Figure 5). The energy gap between the first excited singlet states localized on these Bodipy-based terminals is 0.54 eV (i.e., 4355  $\text{cm}^{-1}$ ). As such, the exciplex is situated at an energy that is intermediate between those of the terminals. Now, illumination into the styryl-bearing Bodipy unit present in **9a–c** results in strong fluorescence from that unit with  $\Phi_F$  and  $\tau_S$  remarkably similar to those recorded for **5**. In contrast, direct

excitation into the yellow-emitting Bodipy unit gives rise to weak fluorescence centered at about 515 nm, together with fluorescence from the opposite terminal (Figure 5). The basic photophysical properties recorded for both terminals in  $\text{Et}_2\text{O}$  are compiled in Table 4. Comparative excitation spectra recorded for emission at 730 nm confirm that photons collected by the yellow-emitting Bodipy chromophore are transferred to the red emitter.

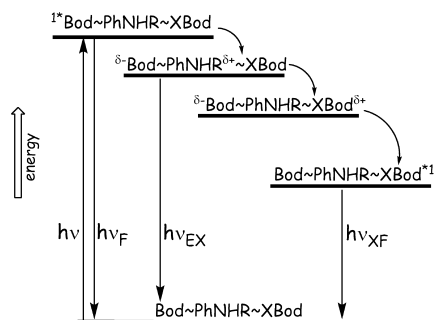
It is usual practice to compute the probability for EET ( $P_{\text{EET}}$ ) by comparing fluorescence lifetimes recorded with and without the acceptor being in place. Unfortunately, the complex emission decay kinetics associated with the Bodipy unit presents problems when this strategy is applied here. Instead,  $P_{\text{EET}}$  values were determined by comparing<sup>29</sup> the excitation spectra with the corresponding absorption spectra recorded in the same solvent and with the same slit width. The values derived in  $\text{Et}_2\text{O}$  are collected in Table 4 and show only a modest dependence on the length of the tether. Indeed,  $P_{\text{EET}}$  decreases from 28% for the shortest tether to 21% for the longest linker. We presume that this drop in EET efficacy relates to the need for large-scale diffusional motion to bring the terminals into close proximity;<sup>30</sup> that is to say, a folded conformation is required for efficient EET.<sup>31</sup> There is a small effect of solvent on the measured  $P_{\text{EET}}$ , with values of 8%, 31%, and 38%, respectively, being found for **9a** in acetonitrile, dioxane, and chloroform. These variations most likely relate to the average conformational distribution present in that solvent and also to the lifetime of the donor. The longer analogues show a similar trend but are always somewhat less efficacious than **9a** under the same conditions. Protonation of the amine by exposure to HCl vapor causes a 40% reduction in  $P_{\text{EET}}$  in each case in  $\text{Et}_2\text{O}$ , this representing a mild form of negative allostery. Under these latter conditions, the exciplex is not formed and it seems likely that the molecular conformation will change. As such, it can be argued that the exciplex assists EET by preorganizing the geometry to some extent.

The question now arises as to whether the exciplex is involved in the EET process as a relay or merely as a spectator that serves to prolong the lifetime of the Bodipy  $S_1$  state via thermal repopulation. There is increased spectral overlap<sup>17d</sup> between exciplex emission and absorption by the expanded Bodipy dye that will favor Förster EET when compared to the case with a conventional Bodipy dye as the donor. Furthermore,  $\tau_{\text{ex}}$  measured at long wavelength in  $\text{Et}_2\text{O}$  is shortened considerably with respect to the corresponding compound lacking the terminal acceptor (e.g., compare **7a** with **9a**), which is entirely consistent with the exciplex fulfilling the role of primary donor. The  $\tau_{\text{ex}}$  values derived from global analysis across a wide spectral range are collected in Table 4 and tend toward a limiting value of 1.25 ns. The shortening of the lifetime can be interpreted in terms of fast EET to the  $S_1$  state localized on the styryl-bearing Bodipy unit, for which the rate constant ( $k_{\text{XT}}$ ) can be estimated (Table 4). This behavior is most unusual. There are prior reports of EET leading to exciplex formation<sup>17f</sup> and one report of exciplex–exciplex annihilation,<sup>17a</sup> but we are unaware of any prior description of EET from an exciplex intermediate. In considering the mechanism of this EET step, we note that  $E_{\text{ox}}$  for the acceptor Bodipy ( $E_{\text{ox}} = 0.72$  V vs SSCE) lies below that of the amine ( $E_{\text{ox}} = 0.98$  V vs SSCE), ignoring the fact that the latter is irreversible in electrochemical terms. As such, EET might proceed by way of charge-transfer interactions along the lines illustrated in Scheme 3.

Addition of potassium ions to a solution of **9a–c** in  $\text{Et}_2\text{O}$  or BuCN had no obvious effect on  $P_{\text{EET}}$ ; hence, there is no

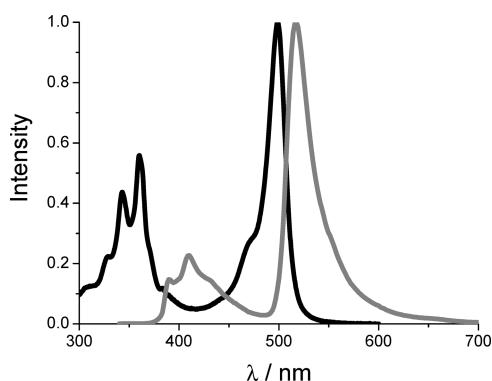
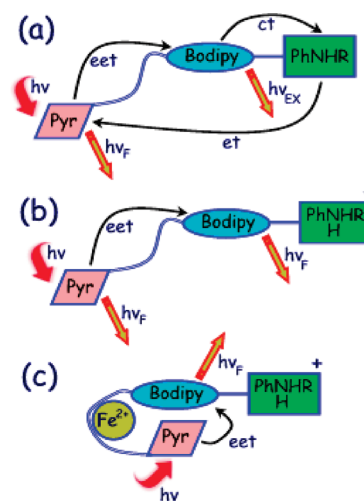
**TABLE 4: Photophysical Properties of the Dual-Dye Systems Recorded in Et<sub>2</sub>O at Room Temperature**

compd	$\lambda_{\text{abs}}/\text{nm}$	$\epsilon_{\text{mzx}}/\text{M}^{-1} \text{ cm}^{-1}$	$\lambda_{\text{flu}}/\text{nm}$	$\Phi_{\text{F}}$	$\tau_{\text{S}}/\text{ns}$ ( $\tau_{\text{ex}}/\text{ns}$ )	$P_{\text{EET}}/\%$	$k_{\text{XT}}/10^7 \text{ s}^{-1}$
<b>9a</b>	646	120000	668	0.51	6.0	28	2.7
	500	86000	514	0.014	(1.25)		
	372	80000					
<b>9b</b>	646	112000	662	0.49	6.0	25	1.7
	501	77000	512	0.030	(1.30)		
	372	74000					
<b>9c</b>	646	107000	665	0.50	5.0	21	1.6
	500	73000	514	0.038	(1.20)		
	371	71000					

**SCHEME 3: Proposed Route for Intramolecular EET Involving the Exciplex as a Direct Intermediate**

allosteric behavior under these conditions. Adding ammonium hexafluorophosphate to a solution of **9c** in  $\text{CHCl}_3$  caused an increase in  $P_{\text{EET}}$  to 92%, which can be explained in terms of the cation folding up the polyethylene glycol chain upon hydrogen bonding to the oxygen atoms. This positive allosteric effect, which brings the terminals into closer proximity, is less pronounced for **9b** ( $P_{\text{EET}}$  increases from 28% to 80%) and nonexistent for **9a** ( $P_{\text{EET}}$  decreases from 26% to 22%). For the longer analogue **9c**, addition of dimethyl sulfoxide disrupted the hydrogen-bonding network formed in the presence of ammonium ions with concomitant loss of the positive allosterism.

**Reverse Energy Transfer Using the Pyrene Derivative.** For the pyrene-linked dye **11** in BuCN direct excitation into the pyrene residue at 362 nm results in a rather weak fluorescence characteristic of the pyrene unit that corresponds to ca. 6% of the fluorescence yield recorded for 1-ethynylpyrene under identical conditions. The emission lifetime measured for the pyrene fluorophore is ca. 0.8 ns, compared to a value of 13.0 ns found for 1-ethynylpyrene. Under the same conditions, fluorescence from the Bodipy unit could be seen clearly (Figure 6); this signal decays as described above. Comparative excitation

**Figure 6.** Absorption (black curve) and fluorescence (gray curve) spectra recorded for **11** in butyronitrile at room temperature. The excitation wavelength was 355 nm.**SCHEME 4: Pictorial Representation of the Events That Follow from Selective Illumination of the Pyrene Chromophore in 11<sup>a</sup>**

<sup>a</sup> Key: (a) normal case, (b) after protonation of the amine, (c) addition of  $\text{Fe}^{2+}$  to the acidified solution.

spectra indicate that EET occurs with a probability of around 45%. Since the overall quenching of pyrene-based emission is almost 95%, it follows that there is an additional nonradiative decay route responsible for about 50% of the initial pyrene  $S_1$  state. This latter process most likely involves electron transfer from the amine to the excited singlet state of pyrene, for which the thermodynamic driving force is ca. 0.26 eV.

Protonation of this amino moiety by exposure to trace amounts of HCl vapor causes an increase in emission from Bodipy, by curtailing exciplex formation, and increases the excited-state lifetime for the pyrene residue to 1.8 ns (Scheme 4). In contrast, adding a small amount of  $\text{Fe}^{2+}$  to the solution decreases  $\tau_{\text{S}}$  for pyrene to only 220 ps while raising  $P_{\text{EET}}$  to ca. 80%, without perturbing the spectral properties. This latter effect must be due to preorganization of the connecting chain so as to bring the terminals into closer proximity (Scheme 4). Addition of trace quantities of both acid and  $\text{Fe}^{2+}$  elevates  $P_{\text{EET}}$  to 95% while rendering Bodipy emission almost quantitative. Neutralization of an acidic solution restores emission to the level seen before addition of acid, while removal of  $\text{Fe}^{2+}$  with adventitious 2,2'-bipyridine reverses this effect.

Since EET is restricted to dipole–dipole interactions in these systems, the level of  $P_{\text{EET}}$  is set by the separation distance<sup>10b</sup> and by the spectral overlap integral.<sup>32</sup> Pyrene-based fluorescence overlaps only weakly with the lowest energy absorption transition localized on Bodipy, but overlap is more pronounced with the transition to the upper singlet excited state. Following EET from pyrene to Bodipy, rapid internal conversion<sup>33</sup> will establish the first excited singlet state localized on Bodipy prior to exciplex formation taking place in the absence of added

protons. For **11** in BuCN at room temperature, the rate constant for intramolecular EET can be estimated as being ca.  $6 \times 10^8 \text{ s}^{-1}$ . From the computed critical distance for EET ( $R_{\text{CC}} = 12.3 \text{ \AA}$ ), the average separation distance between the reactants in the dyad is expected to be ca.  $8.8 \text{ \AA}$ . Preorganization with  $\text{Fe}^{2+}$  decreases this mean separation to ca.  $6.5 \text{ \AA}$ , while the effect of acid is to eliminate electron transfer and improve the emission probability of Bodipy without affecting the properties of the donor. This is a clear illustration of artificial allostereism.

## Conclusion

In this work we describe two separate effects relating to the probability of electronic energy transfer in flexibly linked molecular dyads.

First, the conformation of the connecting chain can be modulated, at least to a modest degree, by external factors. Cation complexation is the obvious choice for this goal<sup>34</sup> and leads to negative or positive allostereism. The effect becomes more pronounced as the chain length increases and could be dramatic for long chains bearing multiple oxygen atoms. There are, of course, other ways to fold up a connecting chain, and these could be used to switch on/off EET in suitably designed dyads. Allostereism of this type is reversible upon removal of the cation or curtailment of complexation. These are not fast events, however, since they require addition of further reagents. Rapid switching of the molecular conformation could be realized by incorporating an electro- or photoactive component in the chain.<sup>35</sup>

The second effect illustrated here relates to involvement of an exciplex as a relay in long-range EET. This is novel behavior that, according to Scheme 3, might demand particular thermodynamic conditions. Formation of the exciplex imposes geometrical changes at the donor center, and in turn, this causes secondary alterations in the alignment of the connecting chain. Such changes are subtle but sufficient to give rise to positive allostereism. Here, the geometry change is fast and does not need the addition of extra reagents. An interesting feature in this respect is that the lifetime of the exciplex can greatly exceed that of the precursor locally excited state;<sup>16</sup> for **9c**, we have observed  $\tau_{\text{ex}}$  as high as 34 ns whereas  $\tau_{\text{S1}}$  does not exceed 5 ns. Such behavior should permit secondary photochemical events to compete effectively with radiative and/or nonradiative deactivation of the excited state. As such, the exciplex might be used to enhance EET in rationally designed dyads.

**Acknowledgment.** This work was supported by the CNRS and Newcastle University. S.M. is grateful to the French Embassy in India for the award of a Sandwich-PhD Scholarship and also to the Bhabha Atomic Research Centre. Dr. Gilles Ulrich is acknowledged for fruitful discussions.

**Supporting Information Available:** Full experimental details and synthesis and characterization of all relevant compounds. This material is available free of charge via the Internet at <http://pubs.acs.org>.

## References and Notes

- (1) Hammarström, L.; Hammes-Schiffer, S. Artificial Photosynthesis and Solar Fuels Special Issue. *Acc. Chem. Res.* **2009**, *42*, 1859–2029.
- (2) Wasielewski, M. R. Reference 1, pp 1910–1920 and references therein.
- (3) Blankenship, R. E. *Molecular Mechanism of Photosynthesis*; Blackwell Science: Oxford, U.K., 2002.
- (4) Aratani, N.; Kim, D.; Osuka, A. Reference 1, pp 1922–1934.
- (5) (a) McDermott, G.; Prince, S. M.; Freer, A. A.; Hawthornthwaite-Lawless, A. M.; Papiz, M. Z.; Cogdell, R. J.; Isaacs, N. W. *Nature* **1995**,

- 374, 517–521. (b) Jean, J. M.; Chan, C. K.; Fleming, G. R. *Isr. J. Chem.* **1988**, *28*, 169–175. (c) Jordanides, X. J.; Scholes, G. D.; Fleming, G. R. *J. Phys. Chem. B* **2001**, *105*, 1652–1669.
- (6) (a) Harriman, A.; Mallon, L. J.; Elliot, K. J.; Haefele, A.; Ulrich, G.; Ziessel, R. *J. Am. Chem. Soc.* **2009**, *131*, 13375–13386. (b) Harriman, A.; Mallon, L. J.; Ziessel, R. *Chem.—Eur. J.* **2008**, *14*, 11461–11473. (c) Goeb, S.; Ziessel, R. *Tetrahedron Lett.* **2008**, *49*, 2569–2574.
- (7) Förster, Th. *Discuss. Faraday Soc.* **1959**, *27*, 7–27.
- (8) (a) Stevens, J. A.; Link, J. J.; Kao, Y. T.; Zang, C.; Wang, L. J.; Zhong, D. P. *J. Phys. Chem. B* **2010**, *114*, 1498–1505. (b) Chatteraj, M.; Bal, B.; Closs, G. L.; Levy, D. H. *J. Phys. Chem.* **1991**, *95*, 9666–9672.
- (9) (a) Head, N. J.; Oliver, A. M.; Look, K.; Lokan, N. R.; Jones, G. A.; Paddon-Row, M. N. *Angew. Chem., Int. Ed.* **1999**, *38*, 3219–3222. (b) Muthiah, C.; Kee, H. L.; Diers, J. R.; Fan, D. Z.; Ptaszek, M.; Bocian, D. F.; Holten, D.; Lindsey, J. S. *Photochem. Photobiol.* **2008**, *84*, 786–801.
- (10) (a) Beljonne, D.; Curutchet, C.; Scholes, G. D.; Silbey, R. J. *J. Phys. Chem. B* **2009**, *113*, 6583–6599. (b) Ziessel, R.; Alamiry, M. A. H.; Elliott, K. J.; Harriman, A. *Angew. Chem., Int. Ed.* **2009**, *48*, 2772–2776. (c) Saini, S.; Srinivas, G.; Bagchi, B. *J. Phys. Chem. B* **2009**, *113*, 1817–1832. (d) Andrews, D. L.; Leeder, J. M. *J. Chem. Phys.* **2009**, *130*, 184504. (e) Wong, K. F.; Bagchi, B.; Rossy, P. J. *J. Phys. Chem. A* **2004**, *108*, 5752–5763. (f) Jiang, Z. J.; Goedel, W. A. *Phys. Chem. Chem. Phys.* **2008**, *10*, 4584–4593. (g) Khan, Y. R.; Dykstra, T. E.; Scholes, G. D. *Chem. Phys. Lett.* **2008**, *461*, 305–309.
- (11) (a) Kovnasyuk, L.; Krämer, R. *Chem. Rev.* **2004**, *104*, 3161–3187. (b) Maier-Peuschel, M.; Frolich, N.; Dees, C.; Hommers, L. G.; Hoffmann, C.; Nikolaev, V. O.; Lohse, M. J. *J. Biol. Chem.* **2010**, *285*, 8793–8800. (c) Zhu, L.; Lynch, V. M.; Anslyn, E. V. *Tetrahedron* **2004**, *60*, 7267–7275. (d) Shepherd, G. B.; Hammes, G. G. *Biochemistry* **1976**, *15*, 311–317.
- (12) (a) Monod, J.; Changeux, J.-P.; Jacob, J.-P. *J. Mol. Biol.* **1963**, *6*, 306–329. (b) Perutz, M. F. *Annu. Rev. Biochem.* **1979**, *48*, 327–386. (c) Perutz, M. F.; Fermi, G.; Luisi, B.; Shaanan, B.; Liddington, R. C. *Acc. Chem. Res.* **1987**, *20*, 309–321. (d) Gramdori, R.; Lavoie, T. A.; Pflumm, M.; Tian, G.; Niersbach, H.; Maas, W. K.; Fairman, R.; Carey, J. J. *Mol. Biol.* **1995**, *254*, 150–162.
- (13) Harriman, A.; Mallon, L. M.; Ulrich, G.; Ziessel, R. *ChemPhysChem* **2007**, *8*, 1207–1214.
- (14) (a) Loudet, A.; Burgess, K. *Chem. Rev.* **2007**, *107*, 4891–1932. (b) Ulrich, G.; Ziessel, R.; Harriman, A. *Angew. Chem., Int. Ed.* **2007**, *47*, 1184–1201. (c) Ziessel, R.; Ulrich, G.; Harriman, A. *New J. Chem.* **2007**, *31*, 496–501.
- (15) Lakowicz, J. R.; Balter, A. *Biophys. Chem.* **1982**, *16*, 117–132.
- (16) (a) Verhoeven, J. W. *Pure Appl. Chem.* **1990**, *62*, 1585–1596. (b) Lewis, F. D.; Cohen, B. E. *J. Phys. Chem.* **1994**, *98*, 10591–10597. (c) Mataga, N.; Chosrowjan, H.; Taniguchi, S. *J. Photochem. Photobiol., C* **2005**, *6*, 37–79.
- (17) (a) Lehtivuori, H.; Lemmetyinen, H.; Tkachenko, N. V. *J. Am. Chem. Soc.* **2006**, *128*, 16036–16037. (b) Mortheani, A. C.; Friend, R. H.; Silva, C. *Chem. Phys. Lett.* **2004**, *391*, 81–84. (c) Kim, J. S.; Seo, B. W.; Gu, H. B. *Synth. Met.* **2003**, *132*, 285–288. (d) Naitou, R.; Ichikawa, M.; Suzuki, T.; Adachi, C.; Koyama, T.; Taniguchi, Y. *Mol. Cryst. Liq. Cryst.* **2001**, *370*, 31–34. (e) Wagner, P. J.; Klan, P. *J. Am. Chem. Soc.* **1999**, *121*, 9626–9635. (f) Bhasikuttan, A. C.; Shastri, L. V.; Sapre, A. V.; Mittal, J. P. *J. Photochem. Photobiol., A* **1998**, *112*, 179–185. (g) Sakamoto, M.; Kim, S. S.; Fujitsuka, M.; Majima, T. *J. Phys. Chem. A* **2008**, *112*, 1403–1407. (h) Teo, Y. N.; Kool, E. T. *Bioconjugate Chem.* **2009**, *20*, 2371–2380.
- (18) Ziessel, R.; Bonardi, L.; Retailleau, P.; Ulrich, G. *J. Org. Chem.* **2006**, *71*, 3093–3102.
- (19) Seo, E. T.; Nelson, R. F.; Fritsch, J. M.; Marcoux, L. S.; Leedy, D. W.; Adams, R. N. *J. Am. Chem. Soc.* **1966**, *88*, 3498–3503.
- (20) (a) Haughland, R. P.; Kang, H. C. U.S. Patent 4,774,339, Sept 27, 1988. (b) Rurack, K.; Kollmansberger, M.; Daub, J. *New J. Chem.* **2001**, *25*, 289–292. (c) Dost, Z.; Atilgan, S.; Akkaya, E. U. *Tetrahedron* **2006**, *62*, 8484–8488. (d) Atilgan, S.; Ekmekci, Z.; Dogan, A. L.; Guç, D.; Akkaya, E. U. *Chem. Commun.* **2006**, 4398–4400. (e) Rurack, K.; Kollmansberger, M.; Resch-Genger, U.; Daub, J. *J. Am. Chem. Soc.* **2000**, *122*, 968–969. (f) Kollmansberger, M.; Rurack, K.; Resch-Genger, U.; Daub, J. *J. Phys. Chem. A* **1998**, *102*, 10211–10220.
- (21) Verhoeven, J. W.; Scherer, T.; Willemsse, R. J. *Pure Appl. Chem.* **1993**, *65*, 1717–1722.
- (22) (a) Masaki, S.; Okada, T.; Mataga, N.; Sakata, Y.; Misumi, S. *Bull. Chem. Soc. Jpn.* **1976**, *49*, 1277–1281. (b) Swinnen, A. M.; van der Auweraer, M.; De schryver, F. C.; Windels, C.; Goedeweck, R.; Vannere, A.; Meeus, F. *Chem. Phys. Lett.* **1983**, *95*, 467–472.
- (23) Bublitz, G. U.; Boxer, S. G. *J. Am. Chem. Soc.* **1998**, *120*, 3988–3992.
- (24) Vath, P.; Zimmt, M. B.; Matyushov, D. V.; Voth, G. A. *J. Phys. Chem. B* **1999**, *103*, 9130–9140.
- (25) (a) Harriman, A.; Heitz, V.; Ebersole, M.; van Willigen, H. *J. Phys. Chem.* **1994**, *98*, 4982–4989. (b) Heitele, H.; Finckh, P.; Weeren, S.;

Pollinger, F.; Michel-Beyerle, M. E. *J. Phys. Chem.* **1989**, *93*, 5173–5178.  
(c) Wasielewski, M. R.; Johnson, D. G.; Svec, W. A.; Kersey, K. M.; Minsek, D. W. *J. Am. Chem. Soc.* **1988**, *110*, 7912–7914.  
(26) (a) Lewis, F. D.; Reddy, G. D.; Bassani, D. M.; Schneider, S.; Gahr, M. *J. Am. Chem. Soc.* **1994**, *116*, 597–605. (b) Scherer, T.; Willemse, R. J.; Verhoeven, J. W. *Recl. Trav. Chim. Pays-Bas* **1991**, *110*, 95–96.  
(27) Leinhos, U.; Kuhnle, W.; Zachariasse, K. A. *J. Phys. Chem.* **1991**, *95*, 2013–2021.  
(28) Brun, A. M.; Harriman, A.; Tsuboi, Y.; Okada, T.; Mataga, N. *J. Chem. Soc., Faraday Trans.* **1995**, *91*, 4047–4057.  
(29) Dirks, G.; Moore, A. L.; Moore, T. A.; Gust, D. *Photochem. Photobiol.* **1980**, *32*, 277–280.  
(30) Price, E. S.; DeVore, M. S.; Johnson, C. K. *J. Phys. Chem. B* **2010**, *114*, 5895–5902.  
(31) Tomschik, M.; Zheng, H. C.; van Holde, K.; Zlatanova, J.; Leuba, S. H. *Proc. Natl. Acad. Sci. U.S.A.* **2005**, *102*, 3278–3283.

(32) Sumi, H. *J. Phys. Chem. B* **1999**, *103*, 252–260.  
(33) Toebe, P.; Zhang, H.; Trieflinger, C.; Daub, J.; Glasbeek, M. *Chem. Phys. Lett.* **2003**, *368*, 66–75.  
(34) (a) Bartoli, S.; De Nicola, G.; Roelens, S. *J. Org. Chem.* **2003**, *68*, 8149–8156. (b) Benniston, A. C.; Harriman, A.; Patel, P. V.; Sams, C. A. *Eur. J. Org. Chem.* **2005**, 4680–4686. (c) Nabeshima, T.; Inaba, T.; Furukawa, N.; Hosoya, T.; Yano, Y. *Inorg. Chem.* **1993**, *32*, 1407–1416. (d) Tung, C. H.; Wu, L. Z. *J. Chem. Soc., Faraday Trans.* **1996**, *92*, 1381–1385.  
(35) (a) Hennrich, G.; Sonnenschein, H.; Resch-Genger, U. *Eur. J. Org. Chem.* **2000**, 539–542. (b) Kang, T. J.; Chang, S. H.; Kim, D. J. *Mol. Cryst. Liq. Cryst.* **1996**, *278*, 181–188. (c) Alobaidi, N. J.; Salam, S. S.; Beer, P. D.; Bush, C. D.; Hamor, T. A.; McQuillan, F. S.; Jones, C. J.; McCleverty, J. A. *Inorg. Chem.* **1992**, *31*, 263–267.

JP106626V